quent treatment of this latter species with excess aqueous Bu^tNH_2 gave **3** in high yield. Compounds **2** and **3** were isolated by concentration of the CH_2Cl_2 solution, drying with $MgSO_4$, filtering off of the $MgSO_4$ and the precipitated $[Bu^tNH_3]Cl$, and then crystallization of the $[Bu^tNH_3]^+$ salts of **2** and **3** by addition of hexane and Et_2O to the filtrate. Spectroscopic data[6,7] indicate that this method consistently gives a product contaminated with 1-2 equiv of $[Bu^tNH_3]Cl$, and a crystal structure (Figure 1) showed the formation of the mixed salt $[Bu^tNH_3]_3[Cp^*WO_3]_2Cl$. The $[Cp^*WO_3]^-$ anion is clearly evident, although with extensive hydrogen bonding to the cation.[8] We have also found that $[Bu^tNH_3][Cp^*WO_3]$ can be obtained free of $[Bu^tNH_3]Cl$ by treatment of $[Cp^*WO_2]_2(\mu\text{-}O)$ (**5**, see below) with Bu^tNH_2/H_2O and that the $[(Ph_3P)_2N]^+$ and $[Bu_4N]^+$ salts can be obtained by metathesis reactions.

Scheme I summarizes the reactions observed for $[Cp^*WO_3]^-$. Preliminary experiments indicate that $[Cp^*MoO_3]^-$ behaves similarly. All of the products illustrated have been isolated as microcrystalline solids and have been spectroscopically characterized.[9-17] Alkylation of **3** with $[Ph_3C]BF_4$ gave the new triphenylmethoxide complex **4**[18] and protonation led to the formation of the known μ-oxo complex **5**,[19] presumably via condensation of initially formed $Cp^*WO_2(OH)$. Complex **3** ring-opened maleic anhydride to give **6**, and it reacted with the heterocumulenes TolN=C=O and PhHC=C=O by [2 + 2] cycloaddition across one of the W=O bonds to give complexes **7** and **8**.[20] For comparison, Herrmann showed that complex **1** underwent a similar [2 + 2] cycloaddition with PhN=C=O, but the ketene Ph_2C=C=O reacted with **1** by [3 + 2] cycloaddition across the ReO_2 unit to give a five-membered metallacycle.[21]

An important consequence of the nucleophilic character of **3** is the ability of its oxo ligands to displace halides from other metals to form heterobimetallic μ-oxo complexes. This is illustrated in Scheme I by the formation of complexes **9-11**. Also illustrated are the addition of $[Cp^*WO_3]^-$ to the electrophilic carbyne carbon of $[Cp(CO)_2Re{\equiv}CTol]^+$ to form the bimetallic carbene complex **13** and the oxidation of **11** to form **12**. These new heterobimetallic species were isolated in excellent yields and have been spectroscopically characterized.[13-17] The formation of **9-13** presages the utility of **2** and **3** for the formation of an extensive series of bimetallic complexes possessing bridging oxo and various oxygenated organic ligands, and studies in those directions are continuing.

Acknowledgment. This research was supported by the National Science Foundation through Grant CHE8802025.

Supplementary Material Available: Tables of atomic positional parameters, selected bond angles and distances, and crystallographic data for $[Bu^tNH_3]_3[Cp^*WO_3]_2Cl$ (5 pages). Ordering information is given on any current masthead page.

(5) Faller, J. W.; Ma, Y. *Organometallics* **1988**, *7*, 559.
(6) **2**: IR (KBr) ν_{MoO} = 860 (vs), 825 (vs) cm^{-1}; ^1H NMR ($CDCl_3$) δ 1.88 (Cp*, 15 H), 1.34 (Bu^t, 25 H); MS (FAB^-), m/z = 281 (M^-).
(7) **3**: IR (KBr) ν_{WO} = 898 (vs), 822 (vs) cm^{-1}; ^1H NMR (CD_2Cl_2) δ 2.01 (Cp*, 15 H), 1.34 (Bu^t, 13 H); MS (FAB^-), m/z = 367 (M^-). Anal. Calcd for $[Bu^tNH_3]_3[Cp^*WO_3]_2Cl$: C, 38.74; H, 6.71. Found: C, 39.08; H, 6.96.
(8) Crystal data for $[Bu^tNH_3]_3[Cp^*WO_3]_2Cl$: $C_{22}H_{51}ClN_3O_3W$, monoclinic, $P2_1/n$, a = 13.822 (4) Å, b = 17.894 (4) Å, c = 17.277 (4) Å, β = 95.06 (2)°, V = 4256.5 (9) Å^3, Z = 4, $R(F)$ = 6.26% on 6352 independent data (3667 observed at $4\sigma F_o$), T = 295 K.
(9) **4**: IR (KBr) ν_{WO} = 923 (m), 915 (m) cm^{-1}; ^1H NMR (CD_2Cl_2) δ 2.06 (Cp*), 7.21-7.31 (Ph); ^{13}C NMR (CD_2Cl_2) δ 147.4 (CPh_3), 119.9 ($C_5(CH_3)_5$), 130.0-127.6 (Ph), 10.8 ($C_5(CH_3)_5$); MS (EI), m/z = 610 (M^+).
(10) **6**: IR (KBr) ν_{CO} = 1718 (m), ν_{WO} = 874 (m), 865 (m) cm^{-1}; ^1H NMR ($CDCl_3$) δ 2.01 (Cp*), 6.14 ($CH{=}CH$); ^{13}C NMR ($CDCl_3$) δ 134.7 ($CH{=}CH$), 168.2 (CO), 120.1 ($C_5(CH_3)_5$), 10.3 ($C_5(CH_3)_5$); MS (FAB^-), m/z = 464 (M^-).
(11) **7**: IR (KBr) ν_{CO} = 1696 (m), ν_{WO} = 937 (s), 892 (s) cm^{-1}; ^1H NMR (CD_2Cl_2) δ 2.14 (Cp*), 2.23 ($TolCH_3$), 7.05-7.20 (aryl); ^{13}C NMR ($CDCl_3$) δ 155.4 (CO), 20.7 ($TolCH_3$), 132.4, 131.9, 120.7, 119.6 (aryl), 120.3 ($C_5(CH_3)_5$), 10.4 ($C_5(CH_3)_5$).
(12) **8**: IR (KBr) ν_{CO} = 1720 (m), ν_{WO} = 937 (s), 891 (s) cm^{-1}; ^1H NMR ($CDCl_3$) δ 2.18 (Cp*), 3.61 (CH), 7.30 (Ph); ^{13}C NMR ($CDCl_3$) δ 45.1 (CHPh), 175.5 (CO), 135.1-126.6 (Ph), 120.3 ($C_5(CH_3)_5$), 10.4 ($C_5(CH_3)_5$); MS (FAB^-), m/z = 485 (M^-).
(13) **9**: IR (KBr) ν_{WO} = 924 (s), 881 (s) cm^{-1}; ^1H NMR ($CDCl_3$) δ 2.14 (Cp*), 6.37 (Cp); ^{17}O NMR (CD_2Cl_2) δ 350.5 (W*O*Zr), 639.8 (W(=*O*)$_2$); MS (FAB), m/z = 623 (M^+). Anal. Calcd for $C_{20}H_{25}O_3ClWZr$: C, 38.50; H, 4.04. Found: C, 38.28; H, 4.19.
(14) **10**: IR (KBr) ν_{WO} = 923 (s), 875 (m) cm^{-1}; ^1H NMR ($CDCl_3$) δ 2.18 (Cp*), 6.42 (Cp); ^{17}O NMR (CD_2Cl_2) δ 449.5 (W*O*Ti), 632.6 (W(=*O*)$_2$); MS (FAB), m/z = 580 (M^+). Anal. Calcd for $C_{20}H_{25}O_3ClTiW$: C, 41.37; H, 4.34. Found: C, 41.16; H, 4.51.
(15) **11**: IR (KBr) ν_{WO} = 904 (m), 849 (m) cm^{-1}; ^1H NMR (CD_2Cl_2) δ 2.12 (Cp*), 4.69 (br, Cp). Anal. Calcd for $C_{20}H_{25}O_3ClVW$: C, 41.16; H, 4.32. Found: C, 41.66; H, 4.65.
(16) **12**: IR (KBr) ν_{WO} = 928 (s), 885 (s) cm^{-1}; ^1H NMR (CD_2Cl_2) δ 2.16 (Cp*), 6.62 (Cp).
(17) **13**: IR (KBr) ν_{CO} = 1946 (vs), 1865 (vs) cm^{-1}, ν_{WO} = 937 (m), 892 (m) cm^{-1}; ^1H NMR (CD_2Cl_2) δ 2.12 (Cp*), 2.30 ($TolCH_3$), 5.34 (Cp), 7.12-7.58 (aryl); ^{13}C NMR (CD_2Cl_2) δ 10.1 ($C_5(CH_3)_5$), 21.2 ($TolCH_3$), 88.7 (C_5H_5), 120.0 ($C_5(CH_3)_5$), 125.3, 128.2, 135.5, 153.2 ($TolC_6H_4$), 203.1 (CO), 280.4 (Re≡*C*).
(18) The compound (tmtaa)Ti=O (tmtaa = 7,6-dihydro-6,8,15,17-tetramethyldibenzo[*b*,*i*][1,4,8,11]tetraazacyclotetradecinato) has also been shown to undergo oxygen alkylation with $[Ph_3C]^+$: Housmekerides, C.; Geoffroy, G. L., unpublished results.
(19) (a) Herrmann, W. A. *J. Organomet. Chem.* **1986**, *300*, 111. (b) Faller, J. W.; Ma, Y. *J. Organomet. Chem.* **1988**, *340*, 59.
(20) The $[(PPh_3)_2N]^+$ salt of **3** was used for the preparation of **8**.
(21) (a) Herrmann, W. A.; Kusthardt, U.; Ziegler, M. L.; Zahn, T. *Angew. Chem., Int. Ed. Engl.* **1985**, *24*, 860. (b) Herrmann, W. A.; Serrano, R.; Kusthardt, U.; Ziegler, M. L.; Guggolz, E.; Zahn, T. *Angew. Chem., Int. Ed. Engl.* **1984**, *23*, 515.

Intracellular Analysis with an Immobilized-Enzyme Glucose Electrode Having a 2-μm Diameter and Subsecond Response Times

T. Abe, Y. Y. Lau, and A. G. Ewing*

Department of Chemistry, 152 Davey Laboratory
Penn State University
University Park, Pennsylvania 16802

Received June 10, 1991

The search for small, rapid, and selective glucose sensors has resulted in a large repertoire of different electrode strategies.[1] Platinized microelectrodes have recently been used with immobilized glucose oxidase to detect glucose with response times of only a few seconds.[2] Pantano et al.[3] recently reported an enzyme-modified microelectrode constructed by linking horseradish peroxidase via a biotin/avidin/biotin tether to carbon fiber electrodes with an 8-μm diameter defining the electroactive surface area and a slightly larger total structural diameter. These electrodes have response times on the order of 300 ms. In this communication, we present a simple procedure to construct enzyme-modified electrodes with total tip diameters as small as 2-μm using platinized carbon ring electrodes.

Carbon ring electrodes were constructed as described previously by Kim et al.[4] The general procedure for immobilizing glucose oxidase on the electrode was similar to that described by Ikariyama et al.[5] Carbon ring electrodes were platinized by reduction of 10 mM hexachloroplatinate in the presence of lead acetate for 3 min. The resulting porous platinum-coated electrodes were then oxidized in phosphate buffer (0.5 M, pH 7.0) at 1.1 V vs a sodium saturated calomel reference electrode (SSCE) for 15 min, oxidized in glucose oxidase (100 mg/mL) for 15 min, and immersed in bovine serum albumin (5% by weight) and finally a gluteraldehyde

* To whom correspondence should be addressed.
(1) (a) Turner, A. P. F.; Karube, I.; Wilson, G. S. In *Biosensors: Fundamentals and Applications*; Oxford University Press: Oxford, 1987. (b) Janata, J. *Anal. Chem.* **1990**, *62*, 33R-44R.
(2) Ikariyama, Y.; Yamauchi, M. A.; Aizwa, M.; Yushiashi, T.; Ushioda, H. *Bull. Chem. Soc. Jpn.* **1988**, *61*, 3525-3530.
(3) Pantano, P.; Morton, T. H.; Kuhr, W. G. *J. Am. Chem. Soc.* **1991**, *113*, 1832-1833.
(4) Kim, Y.-T.; Scarnulis, D. M.; Ewing, A. G. *Anal. Chem.* **1986**, *58*, 1782-1786.
(5) Ikariyama, Y.; Yamauchi, S.; Yukiashi, T.; Ushioda, H. *Anal. Lett.* **1987**, *20*, 1407-1416.

0002-7863/91/1513-7421$02.50/0 © 1991 American Chemical Society

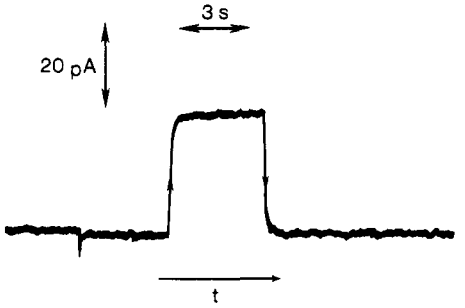

Figure 1. Time course of the amperometric signal observed following a flow injection pulse of 0.5 mM glucose (FIA flow rate, 0.3 μL/min; electrode potential, 0.6 V vs SSCE).

solution (1%) to coat the glucose oxidase with a thin film of albumin and to complete the microsensor.

The microsensor response derives from the amperometric detection of hydrogen peroxide, which is a product of glucose oxidation by the enzyme in the presence of oxygen. The response time of the electrode was determined using flow injection analysis with a stainless steel valve and trap injection system and a 68-μm-i.d. silica capillary. Electrodes coated with glucose oxidase in this manner were checked for stability by observing the signal obtained in static solutions of 3 and 0.5 mM glucose for 20 h. The losses in response over that period of time were found to be 27% and 23%, respectively.

Figure 1 shows the fastest response time obtained with a 2-μm total tip diameter glucose sensor. The rise time[6] is 270 ms, and the fall time is 210 ms. The average response times for glucose microsensors having tip diameters less than 3 μm are 460 ± 190 ms and 430 ± 220 ms for rise and fall times, respectively (n = 4). Interestingly, the response time of these electrodes is observed to increase linearly with electrode tip diameter. Over the range from 2- to 10-μm diameter, the plot of response time vs diameter has a slope of 0.194 s/μm, a correlation coefficient of 0.9022, and an intercept of 0.022 s.

The selectivity of these microsensors was checked in static amperometric experiments by independent injections of enough fructose, galactose, malutose, and KCl (control) to change the solution concentration by 0.1 M. No detectable response was observed. This strongly suggests that the response observed in solutions of glucose is due to oxidation of that substance via glucose oxidase and not due to direct oxidation at the electrode surface.

An important consideration in the use of hydrogen peroxide producing enzyme reactions for amperometric detection is the effect of oxygen concentration on the rate of glucose oxidation via the enzyme. Amperometric detection in a stationary electrochemical cell was used to determine this relationship. Figure 2 shows a plot of the average amperometric signal obtained with glucose microsensors placed in 0.5 mM glucose solution at varied oxygen concentrations. As the concentration of oxygen is reduced from 1 atm to 0 atm, the amperometric response is relatively unaffected until the oxygen concentration is below 0.24 mM. Similar data have been obtained (not shown) for solutions of 50 μM glucose, and no variation is observed until oxygen concentrations as low as 50 μM are reached (3% variation in response at this concentration). This suggests that this type of sensor can be used to monitor glucose in the submillimolar range for experiments where the oxygen level is subject to limited variation, including in vivo analysis.

The development of ultrasmall sensors should eventually make it possible to monitor glucose in the cytoplasm of single functioning cells. Thus, with future developments it might be possible to monitor respiration in single cells of heterogeneous organs (i.e., the brain). Another area of interest is monitoring glucose regulation in single-cell (i.e., liver cells or adipocytes) cytoplasm following administration of cell affectors such as insulin, glucagon,

(6) Response times were evaluated as time for the signal to change from 10% to 90% of full response for rise times and from 90% to 10% for fall times.

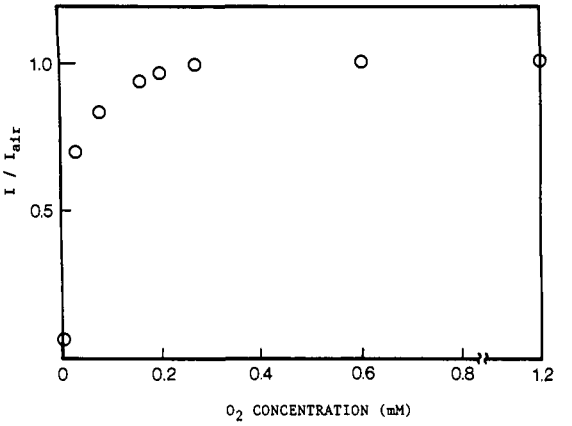

Figure 2. Typical response of a glucose microsensor as a function of oxygen partial pressure. The glucose concentration was 0.5 mM in 0.5 M phosphate buffer at pH 7.0. Oxygen pressure was varied between 0 and 1 atm of oxygen partial pressure. Responses have been normalized to the signal at ambient atmospheric concentration of oxygen.

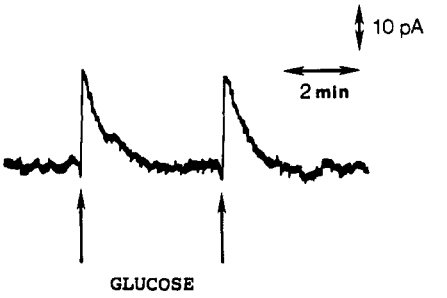

Figure 3. Amperometric current monitored at a 2-μm glucose electrode placed in the cytoplasm of the large dopamine neuron of the pond snail. This neuron has a diameter of approximately 200 μm and a volume of 4–6 nL. The arrows indicate two consecutive injections (2 pL) of 3 M glucose into the cytoplasm. Injections were carried out with an Eppendorf pressure-based microinjector system and a glass micropipet having an approximately 1-μm tip diameter. Injection volumes were approximated by injection of water into oil and measuring the volume optically.

or adrenalin. To determine the applicability of the glucose microsensors developed here, they have been placed into single large dopamine cells of the pond snail, *Planorbis corneus*, and used to measure intentional manipulations of cytoplasmic glucose. Dissection, manipulation, and intracellular voltammetry of neurotransmitters have all been described previously for this cell.[7] Figure 3 shows the intracellular response observed following injections of glucose into the same cell in which a glucose microsensor has been placed. Control experiments have been carried out. No observable change in the amperometric current is observed when either (1) a glucose microsensor is used to monitor injections of phosphate buffer without glucose present or (2) a naked platinized electrode is used intracellularly to monitor cytoplasmic injections of glucose. With the glucose microsensor described, injection of glucose is monitored as a small, but rapid, increase in cytoplasmic levels followed by a more gradual decline, which is likely to represent cellular metabolism and storage of glucose under these conditions. On the basis of in vitro calibrations, the change in cytoplasmic glucose observed in this experiment corresponds to 0.8 mM and the entire response to a transient injection of glucose into the cytoplasm is finished in 2 min.

Despite the bulk-coated enzyme principle by which they are constructed, the glucose oxidase electrodes used here have response times similar to those reported by Pantano et al.,[3] where horseradish peroxidase was covalently attached to the surface of the electrode. It is reasonable to assume that the smaller size of the electrodes reported here offsets the advantages of close localization

(7) (a) Chien, J. B.; Wallingford, R. A.; Ewing, A. G. *J. Neurochem.* **1990**, *54*, 633–638. (b) Lau, Y. Y.; Chien, J. B.; Wong, D. K. Y.; Ewing, A. G. *Electroanalysis (N.Y.)* **1991**, *3*, 87–95.

of the enzyme to the electrode surface gained by a covalent link. Combination of covalent bonding of the enzyme via the biotin/avidin/biotin link described previously[3] with our smaller electrodes[8] might provide response times approaching or less than the 100-ms mark.

Acknowledgment. This work was supported, in part, by the Office of Naval Research. A.G.E. is a recipient of a Presidential Young Investigator Award from the National Science Foundation (CHE-8657193), an Alfred P. Sloan Fellow, and a Camille and Henry Dreyfus Teacher-Scholar.

(8) The total tip diameters of these electrodes range from 2 to 10 μm; however, the thickness of the electroactive ring has been estimated by scanning electron microscopy to be in the range from 50 to 150 nm (Saraceno, R. A.; Ewing, A. G. *J. Electroanal. Chem.* **1988**, *257*, 83-93).

Synthesis and X-ray Crystal Structure of the First Tris(pentamethylcyclopentadienyl)-Metal Complex: $(\eta^5\text{-}C_5Me_5)_3Sm$

William J. Evans,* Shirley L. Gonzales, and Joseph W. Ziller

Department of Chemistry
University of California, Irvine
Irvine, California 92717
Received May 23, 1991

The pentamethylcyclopentadienyl ligand is one of the most broadly utilized ligands in organometallic chemistry.[1-3] This moiety has been complexed to nearly all of the metals in the periodic table, as well as to some non-metals, and the resulting compounds have been investigated extensively. All of these studies have involved molecules containing one or two pentamethylcyclopentadienyl ligands per metal. In no case has a tris(pentamethylcyclopentadienyl) complex been observed, nor was it expected. Due to the large size of the C_5Me_5 ligand, it has been assumed that only two C_5Me_5 groups can coordinate to a single metal atom even for metals as large as the actinides.[4] We report here the synthesis and structure of the first example of a $(\eta^5\text{-}C_5Me_5)_3M$ complex.

As part of our studies of the reactivity of the bent Sm(II) metallocene, $(C_5Me_5)_2Sm$ (**1**), with unsaturated hydrocarbon substrates,[5-8] we examined the reaction of **1** with cyclooctatetraene. On the basis of the strong reduction potential of **1**,[8,9] formation of a complex containing the $C_8H_8^{2-}$ dianion was expected. However, the reaction generated *two* organosamarium products, a red and an orange complex which were separable by sublimation.[10] The less soluble and less volatile red product was identified by X-ray crystallography[11] as the tris(pentamethylcyclopentadienyl) complex, $(\eta^5\text{-}C_5Me_5)_3Sm$ (**2**)[12] (Figure 1). Elemental, chemical, and spectroscopic analysis[13] of the more volatile orange product was consistent with the expected $(C_5Me_5)Sm(C_8H_8)$ (**3**). The THF adduct of **3**, $(C_5Me_5)Sm(C_8H_8)(THF)$, had been previously reported, but since it could not be desolvated,[14] this is the first synthesis of **3**. The stoichiometry of the overall reaction, which occurs immediately upon mixing the reagents in toluene, is shown in eq 1.

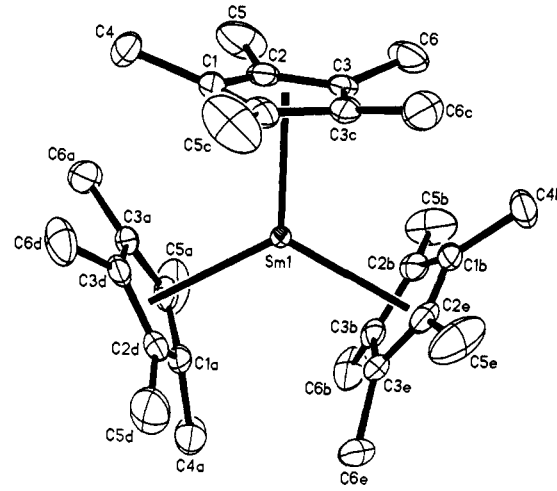

Figure 1. Molecular structure of $(C_5Me_5)_3Sm$ (**2**) with probability ellipsoids drawn at the 50% level.

$$\underset{\mathbf{1}}{2(C_5Me_5)_2Sm} + 1,3,5,7\text{-}C_8H_8 \rightarrow \underset{\mathbf{2}}{(C_5Me_5)_3Sm} + \underset{\mathbf{3}}{(C_5Me_5)Sm(C_8H_8)} \quad (1)$$

Complex **2** crystallizes in space group $P6_3/m$ with crystallographic $\bar{6}$ symmetry at the samarium center. The trigonal coordination geometry around samarium, which is obviously optimal for the three large ligands, is similar to that found in $(C_9H_7)_3Sm$,[16] $[(Me_3Si)_2C_5H_3]_3Sm$,[17] and $Y(OC_6H_3{}^tBu_2\text{-}2,6)_3$,[18] but contrasts with the pyramidal structures found for the complexes $Ln[N(SiMe_3)_2]_3$,[19] $La[CH(SiMe_3)_2]_3$,[20] and $Ce(OC_6H_3{}^tBu_2\text{-}2,6)_3$.[21]

The steric crowding in **2** leads to structural parameters that are beyond the limits previously observed in other pentamethylcyclopentadienyl lanthanide complexes. The average Sm-$C(C_5Me_5)$ bond distance, 2.82 (5) Å, is the longest observed for a trivalent samarium complex,[7] and the individual 2.910 (3) Å Sm-C(1) distance is particularly large. The 120° (ring cen-

(1) (a) King, R. B.; Bisnette, M. B. *J. Organomet. Chem.* **1967**, *8*, 287-297. (b) King, R. B. *Coord. Chem. Rev.* **1976**, *20*, 155-169.
(2) (a) Bercaw, J. E. *Adv. Chem. Ser.* **1978**, *167*, 136-148. (b) Wolczanski, P. T.; Bercaw, J. E. *Acc. Chem. Res.* **1980**, *13*, 121-127. (c) Maitlis, P. M. *Acc. Chem. Res.* **1978**, *11*, 301-307.
(3) *Comprehensive Organometallic Chemistry*; Wilkinson, G., Stone, F. G. A., Abel, E. W., Eds.; Pergamon Press: New York, **1982**.
(4) Tilley, T. D.; Andersen, R. A. *Inorg. Chem.* **1981**, *20*, 3267-3270.
(5) Evans, W. J.; Ulibarri, T. A.; Ziller, J. W. *J. Am. Chem. Soc.* **1990**, *112*, 219-223.
(6) Evans, W. J.; Ulibarri, T. A.; Ziller, J. W. *J. Am. Chem. Soc.* **1990**, *112*, 2314-2324.
(7) Evans, W. J.; Ulibarri, T. A. *J. Am. Chem. Soc.* **1987**, *109*, 4292-4297.
(8) Evans, W. J.; Gonzales, S. L.; Ziller, J. W. In preparation.
(9) Evans, W. J. *Polyhedron* **1987**, *6*, 803-835.
(10) Addition of 1,3,5,7-C_8H_8 (5.7 μL, 0.050 mmol) to a green solution of $(C_5Me_5)_2Sm$ (0.0421 g, 0.100 mmol) in toluene (2 mL) caused immediate formation of a red-brown solution. After the mixture was stirred for 5 min, the solvent was removed by rotary evaporation. Extraction of the red-brown solid with hexane gave a mixture containing a small amount of $(C_5Me_5)_3Sm$ (**2**) and primarily $(C_5Me_5)Sm(C_8H_8)$ (**3**). Extraction of the remaining solid with toluene gave a mixture of primarily **2** with some **3** present. Direct sublimation of the reaction mixture (70 °C, 10^{-4} Torr) yielded **3** as an orange sublimate (18 mg, 93%) and **2** (26 mg, 93%) as a red residue. Both were pure by NMR spectroscopy.
(11) **2** crystallizes from benzene in space group $P6_3/m$ with $a = 9.990$ (1) Å, $c = 15.532$ (2) Å, $V = 1342.5$ Å^3, and $D_{calcd} = 1.375$ g cm^{-3} for $Z = 2$. Least-squares refinement of the model based on 1068 reflections ($|F_o| > 0.0$) converged to a final $R_F = 2.0\%$.
(12) **2**: ^{1}H NMR (C_6D_6) δ -1.24 (br s, C_5Me_5). ^{13}C NMR (C_6D_6) δ 113.16 (C_5Me_5), 28.31 ($C_5\mathit{Me}_5$). IR (KBr) 2958 s, 2910 s, 2861 s, 1438 m, 1378 w, 1263 m, 1099 m, 1021 m, 803 m cm^{-1}. Anal. Calcd for $SmC_{30}H_{45}$: Sm, 27.05; C, 64.80; H, 8.16. Found: Sm, 27.30; C, 64.52; H, 8.03.
(13) **3**: ^{1}H NMR (C_6D_6) δ 8.88 (br s, C_8H_8), 0.65 (C_5Me_5). ^{13}C NMR (C_6D_6) δ 114.32 (C_5Me_5), 85.15 (C_8H_8), 16.88 ($C_5\mathit{Me}_5$). IR (KBr) 2958 m, 2910 m, 2855 m, 1438 w, 1378 w, 1263 m, 1099 m, 1021 m, 893 m, 803 m, 718 s cm^{-1}. Anal. Calcd for $SmC_{18}H_{23}$: Sm, 38.59. Found: Sm, 38.3. Treatment of **3** with THF quantitatively formed $(C_5Me_5)Sm(C_8H_8)(THF)$.[14]
(14) Schumann, H.; Kohn, R. D.; Reier, F.-W.; Dietrich, A.; Pickardt, J. *Organometallics* **1989**, *8*, 1388-1392.
(15) $[(C_5Me_5)La(C_8H_8)]_n$ has been reported: Bruin, P.; Booij, M.; Teuben, J. H.; Oskam, A. *J. Organomet. Chem.* **1988**, *350*, 17-23.
(16) Atwood, J. L.; Burns, J. H.; Lauberau, P. G. *J. Am. Chem. Soc.* **1973**, *95*, 1830-1833.
(17) Evans, W. J.; Keyer, R. A.; Ziller, J. W. *J. Organomet. Chem.* **1990**, *394*, 87-97.
(18) Hitchcock, P. B.; Lappert, M. F.; Smith, R. G. *Inorg. Chim. Acta* **1987**, *139*, 183-184.
(19) (a) Andersen, R. A.; Templeton, D. H.; Zalkin, A. *Inorg. Chem.* **1978**, *17*, 2317-2319. (b) Ghotra, J. S.; Hursthouse, M. B.; Welch, A. J. *J. Chem. Soc., Chem. Commun.* **1973**, 669-670. (c) Eller, P. G.; Bradley, D. C.; Hursthouse, M. B.; Meek, D. W. *Coord. Chem. Rev.* **1977**, *24*, 1-95.
(20) Hitchcock, P. B.; Lappert, M. F.; Smith, R. G.; Bartlett, R. A.; Power, P. P. *J. Chem. Soc., Chem. Commun.* **1988**, 1007-1009.
(21) Stecher, H. A.; Sen, A.; Rheingold, A. L. *Inorg. Chem.* **1988**, *27*, 1132-1133.

0002-7863/91/1513-7423$02.50/0 © 1991 American Chemical Society